Hindawi Publishing Corporation
Advances in Condensed Matter Physics
Volume 2014, Article ID 938072, 5 pages
http://dx.doi.org/10.1155/2014/938072

Research Article

Preparation and Characterization of Novel Fe_2O_3-Flaky Coated Carbon Fiber by Electrospinning and Hydrothermal Methods

Qing-Yun Chen, Lang Liu, and Yun-Hai Wang

International Research Center for Renewable Energy, State Key Laboratory of Multiphase Flow in Power Engineering, Xi'an Jiaotong University, Xi'an 710049, China

Correspondence should be addressed to Qing-Yun Chen; qychen@mail.xjtu.edu.cn

Received 7 March 2014; Accepted 21 May 2014; Published 4 June 2014

Academic Editor: Ke Sun

A novel hierarchical nanostructure of Fe_2O_3-flaky coated carbon fibers was produced by the electrospinning process followed by a hydrothermal technique. First, electrospinning of a colloidal solution that consisted of ferric nitrate and polyacrylonitrile (PAN) was performed to produce PAN nanofibers. Then electrospun nanofiber was stabilized and calcinated in nitrogen at 800°C for 2 h to produce carbon nanofibers (CNFs) which were exploited to produce Fe_2O_3-flaky structure using hydrothermal technique. The as-obtained products were characterized by scanning electron microscopy (SEM) and X-ray diffraction (XRD). The results revealed that Fe_2O_3 flakes were successfully grown on the CNFs substrates, and the coverage of Fe_2O_3 flakes could be controlled by simply adjusting the hydrothermal pH value and time. Fe_2O_3-flaky coated carbon fibers displayed high photocatalytic activity toward degradation of methyl orange (MO) under visible light irradiation.

1. Introduction

Due to the increasing energy crisis and environment problems, an increasing number of scientific researches have focused on the utilization of solar light to split water [1, 2], reduce carbon dioxide (CO_2) [3, 4], and degrade pollutants [5, 6] by photocatalysis. It has been reported that the nanostructured semiconductor metal oxides, such as TiO_2, ZnO, Bi_2O_3, and Fe_2O_3, are effective photocatalysts under visible-light irradiation [7–10]. Among these semiconductor metal oxide photocatalysts, Fe_2O_3, with a low band gap of 2.2 eV, has been recognized as one of the promising materials for photocatalytic process because of its low cost, simple production, environmental friendliness, and excellent chemical stability [11, 12]. However, enhancing the photocatalytic efficiency of Fe_2O_3 to meet the practical application is still a challenge because photoinduced electron-hole pairs in Fe_2O_3 are difficult to be separated.

Recently, the coupling of the photocatalysts and inert supports is one of the approaches to prepare the composite photocatalysts, which may improve charge separation [13, 14]. Mu et al. reported that ZnO-carbon nanofibers (CNFs) showed high photocatalytic property to degrade rhodamine B (RB) [15]. Some reports have shown that CNFs could efficiently capture and transport photoinduced electrons through highly conductive long CNFs [16, 17]. Judging from the promising photocatalyst of Fe_2O_3 and the efficient electron transfer property of CNFs, combination of Fe_2O_3 and CNTs seems to be ideal for improving the photocatalytic efficiency.

In this research, we report a successful attempt for the preparation of carbon fiber which supported Fe_2O_3 nanostructures via the combination of simple electrospinning technique and hydrothermal method, and the photocatalytic activity of these nanostructure photocatalysts is investigated by measuring the degradation of methyl orange (MO) as test substances. The novelty of this study mainly stems from the fabricating of Fe_2O_3-flaky coated carbon nanofibers. The influence factors of the morphology and the structure are discussed in detail.

2. Experiments

2.1. Preparation of Carbon Nanofibers. 2 g of polyacrylonitrile (PAN) (M_w = 150000) was dissolved in 14 mL of N,N-dimethylformamide (DFM) solution containing 3 wt% of

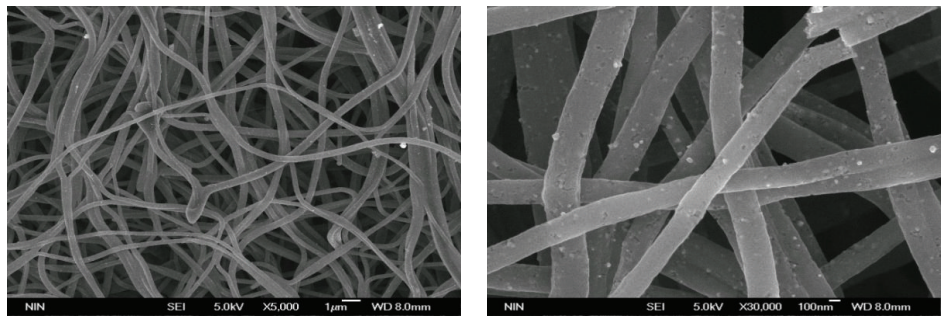

(a) (b)

Figure 1: SEM images of as-obtained carbonized PAN fiber: (a) low magnification and (b) high magnification.

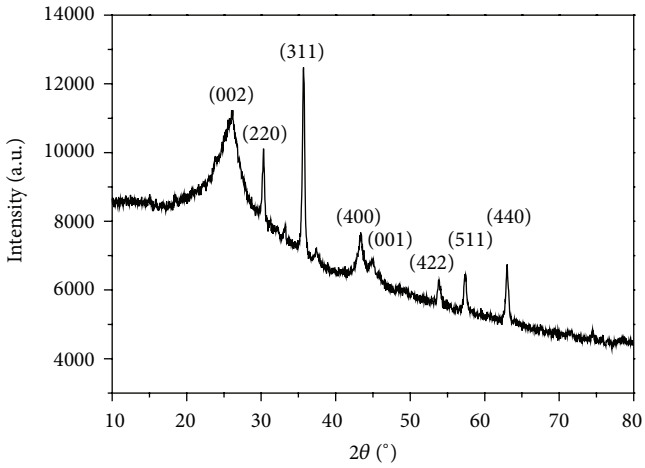

Figure 2: XRD patterns of the as-obtained carbonized PAN fiber.

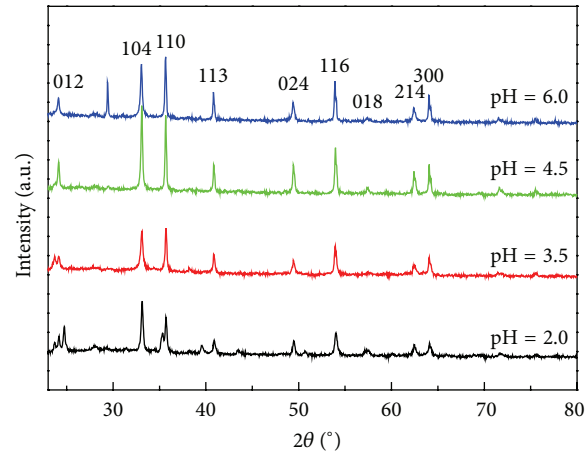

Figure 3: XRD patterns of as-obtained Fe_2O_3-CNFs as the function of pH value.

ferric nitrate. After stirring at room temperature for 6 h, the above precursor solution was transferred into the injection syringe for electrospinning. The positive voltage applied to the needle tip was 25 kV and the distance between the needle tip and aluminum foil as the collector was 14 cm. The as-spun PAN fibers were first stabilized in an air environment at 260°C for 0.5 h and then carbonized in a nitrogen atmosphere at 800°C for 2 h (heating rate of 10°C·min^{-1}).

2.2. Preparation of Fe_2O_3-CNFs Nanostructures. 0.01 g of the obtained CNFs was put into 50 mL of 0.015 M $K_3[Fe(CN)_6]$ solution and dispersed by ultrasound for 30 min. 0.1 M HCl or 0.1 M NaOH solution was dropped into the mixture to adjust the pH value. The obtained mixture was transferred into a 100 mL Teflon-lined stainless steel autoclave, sealed, and maintained at 140°C for different hours and then cooled to room temperature. The as-obtained products were collected, washed several times with distilled water, and then dried at 70°C for 24 h.

2.3. Characterization. The X-ray diffraction (XRD) patterns were recorded by a Panalytical X'pert Pro X-ray diffractometer equipped with CuKa irradiation at a scan rate of 0.02°s^{-1}. The accelerating voltage and the applied current were 40 kV and 40 mA, respectively. The morphology of the samples was determined by field emission scanning electron microscope (SEM, JEOL JSM-6700F). The UV-Vis absorption spectra were measured by a HITACHI UV4100 spectrometer, with the scanning range from 300 nm to 800 nm.

2.4. Photocatalytic Activity. Photocatalytic reaction was carried out in a side-irradiation Pyrex cell at atmospheric pressure and room temperature. The effective irradiation area for the cell is 12.56 cm^2. 0.05 g of photocatalyst powder was dispersed by a stirrer in 100 mL aqueous solution containing 10 mg·l^{-1} MO. The dispersions were sonicated for 60 s and then magnetically stirred in the dark for ca. 15 min to ensure the establishment of adsorption/desorption equilibrium. The photocatalysts were irradiated with visible light through a cutoff filter ($\lambda > 420$ nm) from a 300 W Xe lamp. At a given irradiation time interval, aliquots of 5 mL of the solution were drawn and centrifuged. Subsequently the concentrations of MO in the filtrates were measured quantitatively through the UV-Vis spectrophotometer.

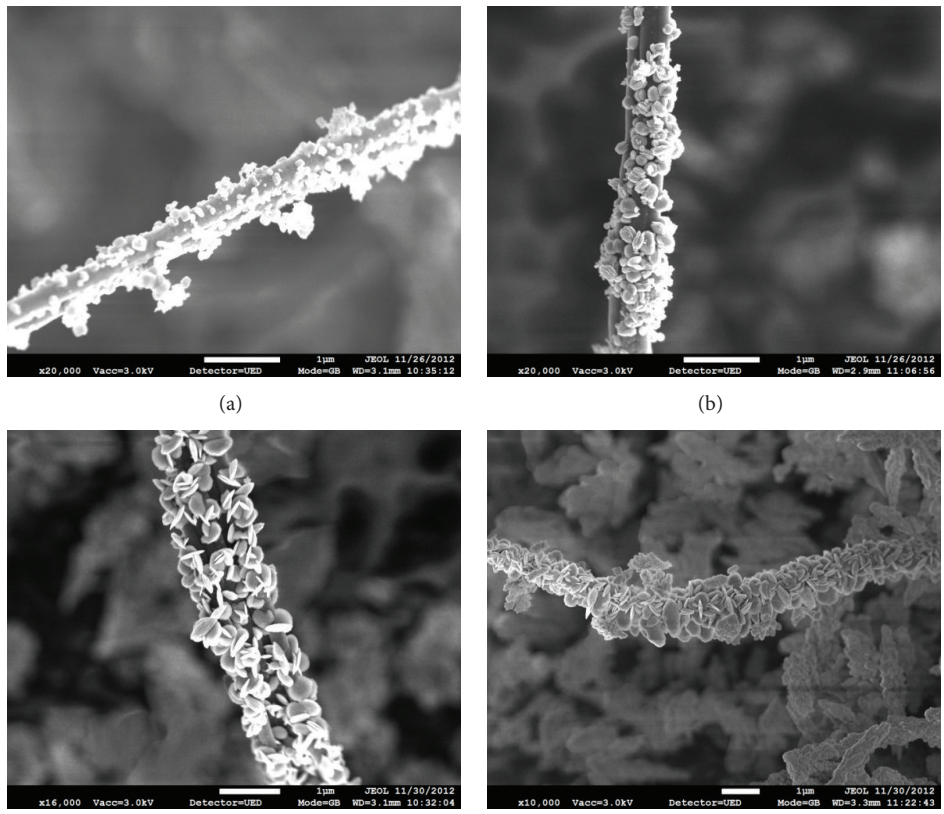

FIGURE 4: SEM images of as-obtained Fe_2O_3-CNFs as the function of pH value: (a) 2.0, (b) 3.5, (c) 4.5, and (d) 6.0.

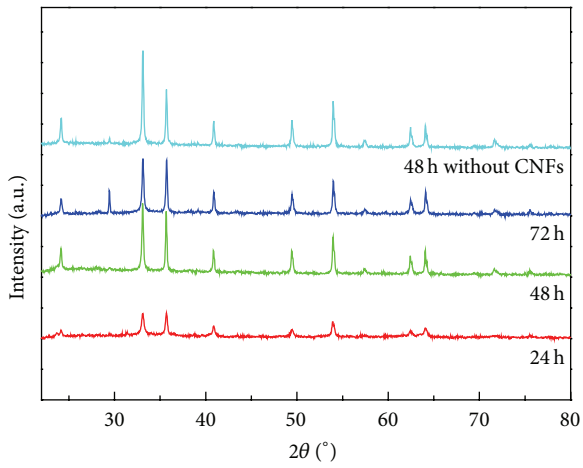

FIGURE 5: XRD patterns of as-obtained Fe_2O_3-CNFs as the function of hydrothermal time.

3. Results and Discussion

Figure 1 shows the SEM images of the carbonized PAN fiber. From Figure 1(a), it can be seen that CNFs align in random orientation because of the bending instability associated with the spinning jet. Figure 1(b) displays the corresponding SEM image with higher magnification. It is shown that these randomly oriented CNFs have a uniform surface with small particles and pores because of the outflow of the Fe_2O_3 particle and small molecule compound during the stabilization and carbonization [18]. The diameter of the CNFs ranges from 300 nm to 500 nm.

The XRD pattern of the as-obtained carbonized PAN fiber is shown in Figure 2. The broad peaks centered at around 26.2° and 43.7° are attributed to the (002) and (010) planes of the graphite carbon structure (JCPDS 41-1487) [19]. The fact that 002 diffraction peaks are relatively low in intensity and broad in shape suggests that as-prepared carbon nanofibers possess low graphitization and crystallization. Also, the broadening of the graphite peaks indicates the existence of some disordered structures in the products. Peaks at 30.3°, 35.7°, 43.3°, 53.8°, 57.4°, and 63.0°, which are corresponding to the diffraction peaks of γ-Fe_2O_3 (JCPDS 25-1402), suggest that nanoparticles are single phase with tetragonal structure [20]. Then these CNFs are exploited to produce Fe_2O_3-CNFs by hydrothermal method.

To investigate the crystal structure of samples obtained from the hydrothermal process, XRD is also performed and the results are shown in Figure 3. The apparent peaks at 24.0°, 33.1°, 35.6°, 40.1°, 49.3°, 53.9°, 57.5°, 62.5°, and 64.0° correspond to the crystal plane of (012), (104), (110), (113), (024), (116), (214), and (300), which confirms the formation of single phase of α-Fe_2O_3 with hexagonal structure (JCPDS 86-0550) [21]. When the pH value is adjusted from 2.0 to 4.5

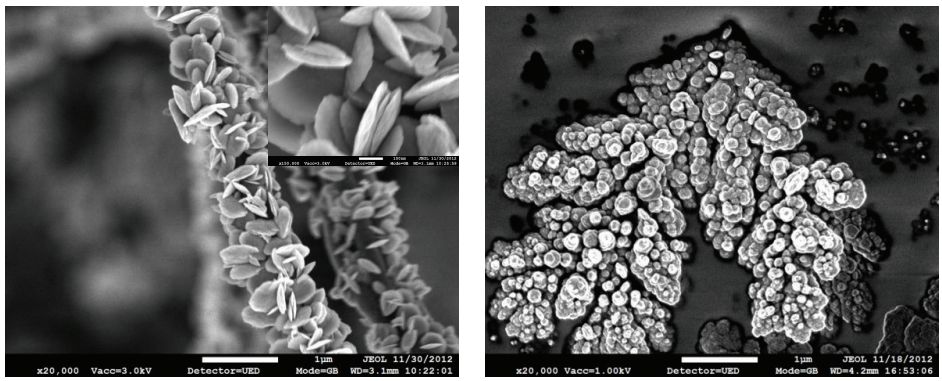

(a) (b)

FIGURE 6: SEM images of (a) as-obtained Fe_2O_3-CNFs (inset is the high magnification of (a)) and (b) Fe_2O_3 without CNFs.

by addition of HCl solution, the peaks belonging to α-Fe_2O_3 phase become sharper and stronger, which indicates that the pH value has a notable effect on the degree of crystallinity. With pH value increasing to 6.0, no significant change for the α-Fe_2O_3 structure is observed. But there appears to be a peak at 30.3 attributed to γ-Fe_2O_3, indicting another phase is formed.

The morphology of the samples obtained from the hydrothermal process as the function of pH value is shown in Figure 4. Obviously, Fe_2O_3 particles have grown on the surface of CNFs and the pH value also has influenced the morphology of Fe_2O_3 particle. At lower pH value, CNFs are coated by the spherical particles that are unevenly distributed. This supports that there are small peaks belonging to carbon at (002) and (010) planes in Figure 3. When pH value increases to 4.5, flaky-shaped particle appears. It may suggest that the intensity of Fe_2O_3 at (110) plane becomes high as seen in Figure 3. From Figure 4(d), we can see that the flaky structure is broken and the as-obtained samples are not uniform in shape at pH value of 6.0. As discussed above, it seems that Fe_2O_3-flaky coated CNFs with good crystallinity can be prepared at pH value of 4.5.

The effect of hydrothermal time on the crystalline structures of Fe_2O_3-CNFs is investigated and the result is shown in Figure 5. As shown in Figure 5, The diffraction peaks of Fe_2O_3, prepared by hydrothermal-treating 48 h, match well with those of pure α-Fe_2O_3, and the intensity of peaks is higher and sharper than that of samples prepared by hydrothermal-treating 72 h and 24 h. When hydrothermal time increases to 72 h, other peaks appear in the XRD patterns which imply the production of impurity phase. Then the best reaction time would be 48 h. In order to compare, Fe_2O_3 powder without CNFs is prepared under the same condition which is the same as the Fe_2O_3-CNFs. From Figure 5, it is found that the same α-Fe_2O_3 is obtained. However, the intensity of (104) and (110) peaks for Fe_2O_3 with or without CNFs is different, which implies that CNFs cause the crystal orientation of Fe_2O_3. Then the corresponding morphology is shown in Figure 6. Obviously, the morphology of Fe_2O_3 is notably affected by adding CNFs. The Fe_2O_3 obtained

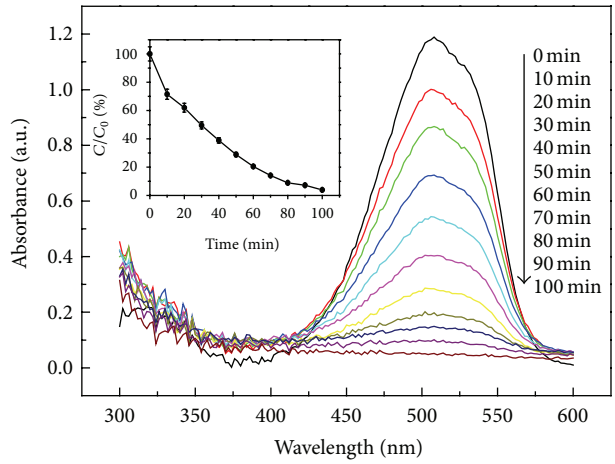

FIGURE 7: Absorption spectra of the solution of MO exposed to irradiation for different time (inset is degradation of MO under visible-light irradiation).

with CNFs has the regular and complete flaky morphology as shown in Figure 6(a). The as-obtained Fe_2O_3 without CNFs is composed of spherical particles and the particles are aggregated as shown in Figure 6(b). This can explain the strong intensity of (110) peaks in XRD patterns. In addition, from Figure 6(a), we can see that the diameter of flakes is about 300 nm. The difference observed in the morphology can be corrected by the XRD pattern.

The photocatalytic activity of as-obtained Fe_2O_3-CNFs prepared under the optimal parameters of pH 4.5 and hydrothermal time of 48 h is evaluated in terms of degradation of MO under irradiation of visible light and the results are shown in Figure 7. It is seen that the intensity of the characteristic adsorption peak of MO solution decreases dramatically in 70 min. Moreover, with the extension of irradiation time, the peak intensity gradually decreases and completely disappears with 100 min irradiation. It reveals that Fe_2O_3-CNFs have an excellent catalytic activity.

4. Conclusion

The α-Fe_2O_3-flaky coated carbon fibers were easily produced by the electrospinning process followed by a hydrothermal technique. The α-Fe_2O_3 flakes with single phase were successfully grown on the CNFs substrates, and the coverage of α-Fe_2O_3 flakes could be controlled by simply adjusting the hydrothermal pH value and time. The optimal parameters for hexagonal α-Fe_2O_3 preparation were pH of 4.5 and hydrothermal time of 48 h. The as-obtained α-Fe_2O_3-CNFs displayed high photocatalytic activity toward degradation of MO under visible-light irradiation. This synthetic method may be promisingly applied in fabricating other bi-multifunctional composites.

Conflict of Interests

The authors declare that there is no conflict of interests regarding the publication of this paper.

Acknowledgments

This work was supported by the Natural Science Foundation of China (NSFC) (nos. 21206133 and 21206134), doctoral program of Chinese Universities (20110201120042), and the National Natural Science Foundation of China, no. 50821064.

References

[1] X. B. Chen, S. H. Shen, L. J. Guo, and S. S. Mao, "Semiconductor-based photocatalytic hydrogen generation," *Chemical Reviews*, vol. 110, no. 11, pp. 6503–6570, 2010.

[2] H. Tong, S. X. Ouyang, Y. P. Bi, N. Umezawa, M. Oshikiri, and J. H. Ye, "Nano-photocatalytic materials: possibilities and challenges," *Advanced Materials*, vol. 24, no. 2, pp. 229–251, 2012.

[3] M. D. Hernández-Alonso, F. Fresno, S. Suárez, and J. M. Coronado, "Development of alternative photocatalysts to TiO_2: challenges and opportunities," *Energy and Environmental Science*, vol. 2, no. 12, pp. 1231–1257, 2009.

[4] J. Mao, K. Li, and T. Y. Peng, "Recent advances in the photocatalytic CO_2 reduction over semiconductors," *Catalysis Science & Techonology*, vol. 3, pp. 2481–2498, 2013.

[5] J. Gong, K. Yao, J. Liu et al., "Striking influence of Fe_2O_3 on the "catalytic carbonization" of chlorinated poly(vinyl chloride) into carbon microspheres with high performance in the photodegradation of Congo red," *Journal of Materials Chemistry A*, vol. 1, no. 17, pp. 5247–5255, 2013.

[6] D. Chatterjee and S. Dasgupta, "Visible light induced photocatalytic degradation of organic pollutants," *Journal of Photochemistry and Photobiology C: Photochemistry Reviews*, vol. 6, no. 2-3, pp. 186–205, 2005.

[7] Q.-Y. Chen, J.-S. Liu, Y. Liu, and Y.-H. Wang, "Hydrogen production on TiO_2 nanorod arrays cathode coupling with bioanode with additional electricity generation," *Journal of Power Sources*, vol. 238, pp. 345–349, 2013.

[8] F. L. Zhou, X. J. Li, J. Shu, and J. Wang, "Synthesis and visible light photo-electrochemical behaviors of In_2O_3-sensitized ZnO nanowire array film," *Journal of Photochemistry and Photobiology A: Chemistry*, vol. 219, no. 1, pp. 132–138, 2011.

[9] Z. F. Bian, J. Zhu, S. H. Wang, Y. Cao, X. F. Qian, and H. X. Li, "Self-assembly of active Bi_2O_3/TiO_2 visible photocatalyst with ordered mesoporous structure and highly crystallized anatase," *Journal of Physical Chemistry C*, vol. 112, no. 16, pp. 6258–6262, 2008.

[10] G. Liu, Q. Deng, H. Wang et al., "Micro/nanostructured α-Fe_2O_3 spheres: synthesis, characterization, and structurally enhanced visible-light photocatalytic activity," *Journal of Materials Chemistry*, vol. 22, no. 19, pp. 9704–9713, 2012.

[11] Y. Shi, H. Y. Li, L. Wang, W. Shen, and H. Z. Chen, "Novel α-Fe_2O_3/CdS cornlike nanorods with enhanced photocatalytic performance," *ACS Applied Materials and Interfaces*, vol. 4, no. 9, pp. 4800–4806, 2012.

[12] L. MacHala, J. Tuček, and R. Zbořil, "Polymorphous transformations of nanometric iron(III) oxide: a review," *Chemistry of Materials*, vol. 23, no. 14, pp. 3255–3272, 2011.

[13] S. Kedem, D. Rozen, Y. Cohen, and Y. Paz, "Enhanced stability effect in composite polymeric nanofibers containing titanium dioxide and carbon nanotubes," *Journal of Physical Chemistry C*, vol. 113, no. 33, pp. 14893–14899, 2009.

[14] H. Yu, X. Quan, S. Chen, and H. Zhao, "TiO_2-multiwalled carbon nanotube heterojunction arrays and their charge separation capability," *Journal of Physical Chemistry C*, vol. 111, no. 35, pp. 12987–12991, 2007.

[15] J. B. Mu, C. L. Shao, Z. C. Guo et al., "High photocatalytic activity of ZnO-carbon nanofiber heteroarchitectures," *ACS Applied Materials and Interfaces*, vol. 3, no. 2, pp. 590–596, 2011.

[16] J. Liu, J. Li, A. Sedhain, J. Lin, and H. Jiang, "Structure and photoluminescence study of TiO_2 nanoneedle texture along vertically aligned carbon nanofiber arrays," *Journal of Physical Chemistry C*, vol. 112, no. 44, pp. 17127–17132, 2008.

[17] H. E. Unalan, D. Wei, K. Suzuki et al., "Photoelectrochemical cell using dye sensitized zinc oxide nanowires grown on carbon fibers," *Applied Physics Letters*, vol. 93, no. 13, Article ID 133116, 2008.

[18] L. W. Ji, O. Toprakci, M. Alcoutlabi et al., "α-Fe_2O_3 nanoparticle-loaded carbon nanofibers as stable and high-capacity anodes for rechargeable lithium-ion batteries," *ACS Applied Materials and Interfaces*, vol. 4, no. 5, pp. 2672–2679, 2012.

[19] Y. L. Luo, Q. Y. Chen, D. Zhu, and M. Matsuo, "Graphite carbon foam films prepared from porous polyimide with in situ formed catalytic nickel particles," *Journal of Applied Polymer Science*, vol. 116, no. 4, pp. 2110–2118, 2010.

[20] S.-Z. Guo, Y. Li, J.-S. Jiang, and H.-Q. Xie, "Nanofluids containing γ-Fe_2O_3 nanoparticles and their heat transfer enhancements," *Nanoscale Research Letters*, vol. 5, no. 7, pp. 1222–1227, 2010.

[21] L. X. Yang, Y. Liang, H. Chen, L. Y. Kong, and W. Jiang, "Facile hydrothermal route to the controlled synthesis of α-Fe_2O_3 1-D nanostructures," *Bulletin of Materials Science*, vol. 31, no. 7, pp. 919–923, 2008.